

Synthesis of pH- and temperature-responsive chitosan-graft-poly[2-(*N,N*-dimethylamino)ethyl methacrylate] copolymer and gold nanoparticle stabilization by its micelles

Weizhong Yuan,^{a,b*} Zhengda Zhao,^a Jinying Yuan,^c Shuying Gu,^{a,b} Fengbo Zhang,^d Xuming Xie^d and Jie Ren^{a,b}

Abstract

Novel pH- and temperature-responsive chitosan-graft-poly[2-(*N,N*-dimethylamino)ethyl methacrylate] (chitosan-g-PDMAEMA) copolymers were successfully synthesized by homogeneous atom transfer radical polymerization (ATRP) under mild conditions. Chitosan macroinitiator was prepared by phthaloylation of amino groups of chitosan and subsequent acylation of hydroxyl groups of chitosan with 2-bromoisobutyryl bromide. The copolymers were obtained by ATRP of 2-(*N,N*-dimethylamino)ethyl methacrylate and they can self-assemble into stable micelles in water. Hybrid micelles with a PDMAEMA corona incorporating gold nanoparticles (Au NPs) were prepared *in situ* via the reduction of HAuCl₄ with NaBH₄. The pH and temperature responses of the copolymer micelles and hybrid micelles were characterized using UV-visible spectroscopy and dynamic laser light scattering. The morphology of the micelles was observed using transmission electron microscopy and atomic force microscopy. The PDMAEMA corona of the micelles acts as the 'nanoreactor' and the 'anchor' for the *in situ* formation and stabilization of Au NPs. Therefore, the spatial distribution of Au NPs within the micelles can be tuned by varying the temperature and pH value.

© 2010 Society of Chemical Industry

Keywords: chitosan-graft-poly[2-(*N,N*-dimethylamino)ethyl methacrylate]; gold nanoparticle stabilization; pH- and temperature-responsive hybrid micelles

INTRODUCTION

Considerable attention has been paid to the exploration of metal nanoparticles (NPs) due to their unique properties and applications in fields ranging from optoelectronics and sensors to catalysis and medicine.^{1–12} Much research has involved the fabrication of NP assemblies because they represent a popular route towards the preparation of advanced functional materials as well as a central concept in nanoscience and nanotechnology.^{13–15} Among noble metal NPs, gold NPs (Au NPs) have attracted special interest owing to their advantages in areas such as photosensitivity, catalysis, medical diagnosis and biomedical imaging.^{16–20}

In order to prevent the aggregation of metal NPs caused by their high surface energy, they must be stabilized in solution or in a matrix. To this end, polymer-NP composites are promising candidates with the purpose of exploiting or enhancing the properties of NPs; the polymer matrix can control host-guest interactions to ensure the well-defined spatial distribution of NPs. To date, a great many carrier systems have been developed for the stabilization of metal NPs, such as dendrimers,^{21,22} latex particles,^{23–25} microgels^{26–28} or block copolymer micelles.^{29–32} In general, the polymer matrix only serves as a scaffold for immobilizing the NPs and preventing them from aggregation. However, it would be highly desirable to be able to modulate the spatial distribution of NPs arising from a change in polymer chain conformation in response to some external chemical or biochemical species in some specific applications. Liu and co-workers

reported the *in situ* formation of Ag NPs with tunable spatial distribution at the thermosensitive poly(*N*-isopropylacrylamide) (PNIPAAm) corona of dendritic unimolecular micelles.³³ Gupta *et al.* reported a facile route for the stabilization of Ag NPs and Au NPs onto pH-responsive poly(2-vinylpyridine) (P2VP) brushes.^{34,35} Chen *et al.* reported the anchoring of Au NPs to pH-responsive poly(4-vinylpyridine) (P4VP) blocks of poly(ethylene glycol)-block-polystyrene-block-poly(4-vinylpyridine) (PEG-*b*-PST-*b*-P4VP) copolymers and the formation of core-shell-corona Au-micelle composites with a tunable smart hybrid shell.³⁶ Zhang and co-workers reported the fabrication of Au NPs on a template

* Correspondence to: Weizhong Yuan, Institute of Nano- and Bio-polymeric Materials, School of Materials Science and Engineering, Tongji University, Shanghai 20092, People's Republic of China. E-mail: yuanwz@tongji.edu.cn

a Institute of Nano- and Bio-polymeric Materials, School of Materials Science and Engineering, Tongji University, Shanghai 20092, People's Republic of China

b Key Laboratory of Advanced Civil Engineering Materials of Ministry of Education, Shanghai 20092, People's Republic of China

c Key Laboratory of Organic Optoelectronics and Molecular Engineering of Ministry of Education, Department of Chemistry, Tsinghua University, Beijing 100084, People's Republic of China

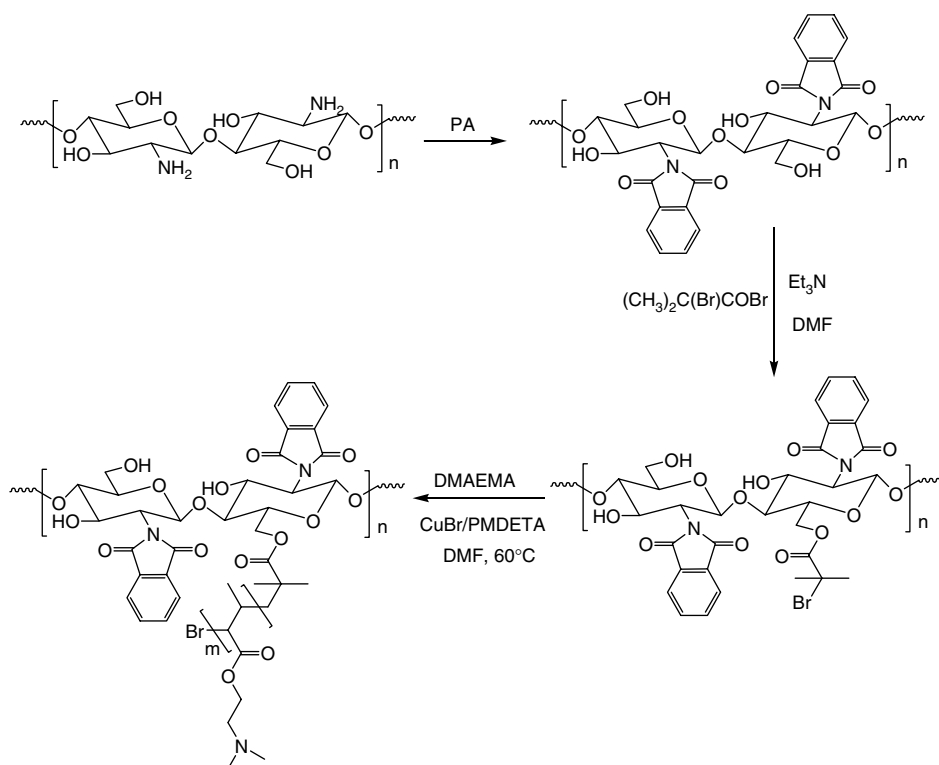
d Department of Chemical Engineering, Tsinghua University, Beijing 100084, People's Republic of China

of the thermoresponsive and pH-responsive coordination triblock copolymer PEG-*b*-P4VP-*b*-PNIPAAm.³⁷ Chen and co-workers reported the core-shell reversion of hybrid PSt-*b*-P4VP polymeric micelles containing Au NPs in the core.³⁸ Gauthier and co-workers reported the *in situ* formation of Au NPs with amphiphilic PSt-*g*-(P2VP-*b*-PSt) copolymer as the template.³⁹ Liu and co-workers reported the fabrication of Au NPs on pH-responsive poly[(2-(*N,N*-dimethylamino)ethyl methacrylate] (PDMAEMA) brushes on the surface of colloid particles.⁴⁰ McCormick and co-workers reported the *in situ* formation of Au NP-decorated vesicles from thermally responsive PDMAEMA-*b*-PNIPAAm block copolymer.⁴¹ These polymeric matrixes can be used to adjust the spatial distribution between NPs arising from the change in polymer chain conformation in response to a change of surrounding temperature or pH value. Therefore, they have many applications such as in biocatalysis, biosensors, biotesting and protein adsorption. However, most of these polymers are complicated to prepare and their micelles tend to disintegrate upon change of external conditions. When hydrophilic and responsive polymer chains are tethered to a hydrophobic multifunctional chain, such as graft copolymers, they can serve as highly stable and responsive templates for the preparation of hybrids of polymer and metal nanoparticles.

Recently, as an abundant natural biomaterial, chitosan has attracted much interest due to its good biocompatibility, biodegradability, non-toxicity and bioactivity, and therefore has found wide application in the biomedical field.^{42–48} The grafting modification of chitosan has been explored as a convenient method to overcome its insolubility in common solvents and develop multifunctional novel hybrid materials.^{49–53} Feng and Dong reported the preparation of chitosan-*graft*-poly(ϵ -caprolactone) and chitosan-*graft*-poly(L-lactide) (chitosan-*g*-PLLA) by ring-opening polymerization.^{54,55} Chitosan-*g*-PLLA can self-assemble into

micelles in aqueous solution. Yu *et al.* reported the preparation of chitosan-*graft*-poly(L-lysine) for gene transfection.⁵⁶ Bai and co-workers reported the preparation of chitosan beads grafted with polyacrylamide via surface-initiated atom transfer radical polymerization (ATRP) for enhanced and selective absorption of mercury ions.⁵⁷ Obviously, amphiphilic chitosan graft copolymers can be prepared with facile methods and the relative graft-chain lengths as well as composition are adjustable with 'living'/controlled polymerization. More importantly, amphiphilic chitosan graft copolymers can form stable micelles and serve as highly stable templates for the preparation of hybrids containing metal NPs due to their well-defined chemical structures with grafted chains of controllable length.

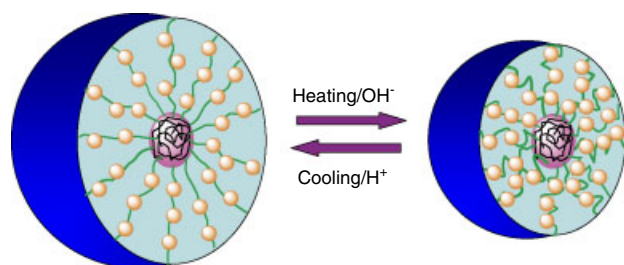
Herein, we report the employment of pH- and temperature-responsive graft copolymer micelles as templates for the *in situ* preparation and stabilization of Au NPs with controllable spatial distribution. Amphiphilic chitosan-*g*-PDMAEMA copolymers were synthesized by ATRP (Scheme 1). Au NPs were generated and stabilized *in situ* at the pH- and temperature-responsive shell of graft copolymer micelles (Scheme 2). The core of the micellar carrier consists of chitosan chains and the shell consists of grafted PDMAEMA chains. Controlling the spatial distribution of Au NPs inside the graft copolymer micelles is achieved by taking advantage of the phase transition of the PDMAEMA corona at its lower critical solution temperature (LCST) or pH values of surrounding aqueous media. At low temperatures or pH values, the PDMAEMA shell shows swelling behavior and the stabilized NPs are fully accessible to external chemical and biochemical species; at high temperature or pH values, the polymer shell shows deswelling behavior. In the latter case, the spatial distance between Au NPs decreases and the permeability of the PDMAEMA corona reduces considerably (Scheme 3).



Scheme 1. Synthesis of chitosan-*g*-PDMAEMA graft copolymer by ATRP.



Scheme 2. *In situ* formation and immobilization of Au NPs onto PDMAEMA chains of chitosan-*g*-PDMAEMA graft copolymer micelles.



Scheme 3. Hybrid chitosan-*g*-PDMAEMA graft copolymer micelles exhibiting thermo- or pH-tunable spatial distances between Au NPs.

EXPERIMENTAL

Materials

Chitosan (viscosity = 200 cP, degree of deacetylation = 80%) was purchased from Aldrich and dried *in vacuo* at 60 °C for 12 h before use. Phthalic anhydride (PA) was used as received. DMAEMA (Acros Organic, USA) was dried over CaH₂ and distilled under reduced pressure. CuBr was purified by stirring in acetic acid and washing with ethanol and then dried *in vacuo*. Pentamethylenetriamine (PMDTA; Acros Organic, USA) was stirred overnight with CaH₂ and distilled under reduced pressure. 2-Bromoisobutyryl bromide (Aldrich, USA) was distilled under reduced pressure. *N,N*-dimethylformamide (DMF) was dried over CaH₂ and distilled under reduced pressure. HAuCl₄ · 4H₂O and NaBH₄ (Sinopharm Chemical Reagent Co. Ltd, Shanghai, China) were used as received.

Characterization

Attenuated total internal reflectance Fourier transform infrared (ATR-FTIR) spectra of samples were recorded with an EQUINOSS/HYPERION2000 spectrometer (Bruker, Germany). ¹H NMR spectra of samples were obtained using a Bruker DMX 500 NMR spectrometer with deuterated dimethylsulfoxide (DMSO-*d*₆) and D₂O as solvents. The chemical shifts were relative to tetramethylsilane.

For turbidity measurements, the light transmittance of graft copolymer micellar solutions was monitored as a function of pH or temperature at a fixed wavelength of 500 nm by means of a Lambda 35 UV-visible spectrophotometer (PerkinElmer, USA) equipped with a circulating water bath. An aqueous copolymer solution concentration of 15 g L⁻¹ was used. To investigate the effect of temperature variation, the operation was conducted with a programmed temperature increase from 35 to 65 °C at a rate of 1 °C (20 min)⁻¹.

UV-visible absorption spectra were recorded with a computer-controlled Lambda 35 UV-visible spectrophotometer.

The morphology of micelles of chitosan-*g*-PDMAEMA graft copolymers and hybrid micelles in water was investigated using the dynamic laser light scattering (DLS) technique. The experiments were performed with a Malvern Autosizer 4700 DLS spectrometer. DLS was performed at a scattering angle 90°. The hydrodynamic radius was obtained by a cumulant analysis.

The morphology of copolymer micelles and hybrid micelles was observed with a JEOL JEM-2010 transmission electron microscopy (TEM) instrument at an accelerating voltage of 120 kV. The samples for TEM observation were prepared by placing 10 μL of copolymer micelle or hybrid micelle solution on copper grids coated with thin films of carbon.

AFM observations were conducted with an SPM-9500J3 atom force microscope (Shimadzu, Japan). Sample preparation was similar to that for TEM analyses, but transparent mica was used as the substrate.

Synthesis of chitosan-Br macroinitiator

Chitosan was heated with excess PA in anhydrous DMF to give phthaloyl-chitosan according to a previously reported procedure.⁴³ It was obtained as a light-yellow powdery material after drying *in vacuo*. Then, the dried phthaloyl-chitosan (5 g, 17.6 mmol of GlcN units) was completely dissolved in anhydrous DMF (100 mL) under stirring. To this solution was added triethylamine (2.19 g, 22 mmol) under nitrogen at room temperature. The mixture was stirred and cooled to 0 °C with an ice bath. Then, 2-bromoisobutyryl bromide (5 g, 22 mmol) in anhydrous DMF (20 mL) was added dropwise to the mixture over a period of 40 min. The reaction mixture was stirred for 12 h at room temperature before it was washed with saturated NaHCO₃ aqueous solution and deionized water. The chitosan-Br macroinitiator powder was obtained by filtration and dried *in vacuo*.

Phthaloyl-chitosan. FTIR (KBr; cm⁻¹): 3300–3600 (ν_{O-H}), 2930 (ν_{C-H}), 1772 and 1709 (phthalimido groups), 721 (aromatic ring). ¹H NMR (DMSO-*d*₆; δ, ppm): 7.37–7.90 (m, aromatic protons), 2.56–5.62 (m, protons of chitosan chain).

Chitosan-Br. FTIR (KBr; cm⁻¹): 3300–3590 (ν_{O-H}), 2930 (ν_{C-H}), 1772 and 1709 (phthalimido groups), 1740 (ν_{C=O}), 721 (aromatic ring). ¹H NMR (DMSO-*d*₆; δ, ppm): 7.39–7.91 (m, aromatic protons), 2.56–5.62 (m, protons of chitosan chain), 1.86 (s, OCOC(CH₃)₂Br).

Synthesis of chitosan-*g*-PDMAEMA copolymer

In a general procedure, chitosan-Br macroinitiator (0.1 g, 62.5 μmol of C–Br) was dissolved in anhydrous DMF (10 mL) and added with CuBr (9 mg, 62.5 μmol) and DMAEMA (3.93 g, 25 mmol) into a dried flask with a magnetic stirring bar. The reaction system was degassed with three freeze–evacuate–thaw cycles and then deoxygenated PMDETA (13.5 μL, 62.5 μmol) was introduced into the flask using a syringe under a nitrogen atmosphere. The reaction was then performed at 60 °C for 4 h. The polymerization was stopped by exposing the mixture to air and diluting with deionized water. The mixture was then dialyzed in a dialysis bag (molecular weight cutoff of 8000–10 000 g mol⁻¹) against deionized water for 96 h. It was refreshed at intervals of 6 h.

FTIR (KBr; cm⁻¹): 2943 and 2800 (ν_{C-H}), 1726 (ν_{C=O}). ¹H NMR (D₂O; δ, ppm): 3.79–4.26 (m, COOCH₂ in PDMAEMA), 2.51–2.75 (m, CH₂N(CH₃)₂), 2.09–2.36 (m, CH₂N(CH₃)₂), 1.63–1.93 (m, CH₂ in PDMAEMA), 0.59–1.11 (m, CH₃ in PDMAEMA).

Stabilization of Au NPs by chitosan-*g*-PDMAEMA micelles

The *in situ* formation and stabilization of Au NPs by graft copolymer micelles was carried out by the addition of HAuCl₄ · 4H₂O solution into an aqueous chitosan-*g*-PDMAEMA solution and subsequent reduction with NaBH₄. As a typical example, 133.5 mg of chitosan-*g*-PDMAEMA was dissolved in 8.9 mL of deionized water, and an aqueous solution of 6.6 × 10⁻³ mol L⁻¹ of HAuCl₄ · 4H₂O (2.71 mL) was then added. After gently stirring for 30 min, the solution was subjected to dialysis against deionized water for 30 min. An aliquot of an aqueous solution of NaBH₄ (0.03 mol L⁻¹, 1.18 mL) was then quickly added, and stirring was continued for 2 h. The Au NP hybrid composite solution was further purified by dialysis against deionized water for 24 h at room temperature.

RESULTS AND DISCUSSION

Preparation of chitosan-Br macroinitiator and chitosan-*g*-PDMAEMA copolymer

Chitosan can be easily converted to phthaloyl-chitosan by the phthaloylation of amino groups of chitosan. Introduction of phthaloyl groups can reduce the inter- or intramolecular hydrogen bonds, which results in the solubility of chitosan in organic solvents such as DMSO and DMF. Thus, this will facilitate the reaction of hydroxyl groups of chitosan with 2-bromoisobutyryl bromide under homogeneous conditions. Compared to the FTIR spectrum of chitosan (Fig. 1(a)), that of phthaloyl-chitosan shows the characteristic peaks at 1772 and 1709 cm⁻¹ of the phthalimido groups and at 721 cm⁻¹ of aromatic rings (Fig. 1(b)). The degree of substitution of phthaloyl groups within phthaloyl-chitosan is determined to be about 1.1 from ¹H NMR analysis (Fig. 2(a)). This suggests that all the amino groups of chitosan completely reacted with PA.

The chitosan-Br macroinitiator of ATRP was obtained by the reaction of phthaloyl-chitosan with 2-bromoisobutyryl bromide under homogeneous conditions. The formation of chitosan-Br was confirmed from FTIR and ¹H NMR analysis. In the FTIR spectrum (Fig. 1(c)), the absorption band at about 1740 cm⁻¹ corresponding to carbonyl group of chitosan-Br appears, indicating that 2-bromoisobutyryl groups had been introduced onto chitosan chains. The absorption band of carbonyl groups of chitosan-Br is not obvious due to the overlap of the band of phthalimido

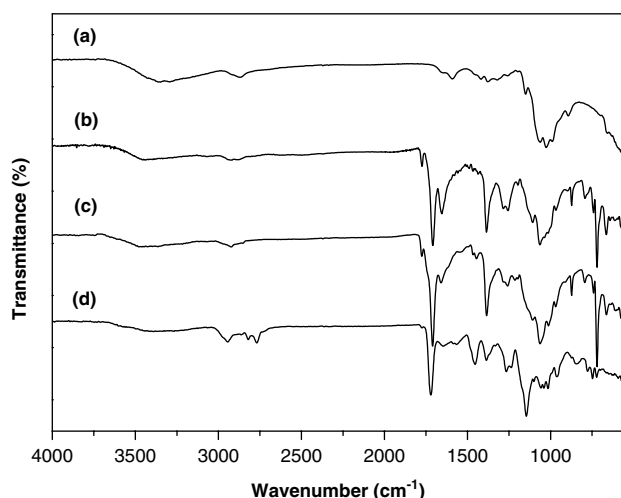


Figure 1. FTIR spectra of (a) chitosan, (b) phthaloyl-chitosan, (c) chitosan-Br and (d) chitosan-*g*-PDMAEMA2.

groups. However, the ¹H NMR spectrum can clarify the presence of 2-bromoisobutyryl groups. The ¹H NMR spectrum of chitosan-Br is shown in Fig. 2(b). The novel signal corresponding to methyl protons of 2-bromoisobutyryl groups appears at 1.85 ppm, which further indicates that the hydroxyl groups have been reacted. The degree of substitution of 2-bromoisobutyryl groups within chitosan-Br is determined to be 0.1 from ¹H NMR analysis (Fig. 2(b)).

Chitosan-*g*-PDMAEMA copolymers were prepared from chitosan-Br macroinitiator and DMAEMA via ATRP at 60 °C. DMF was used as the solvent to ensure a homogeneous reaction solution, which is important to obtain a uniform distribution of grafting polymerization in the chitosan macromolecules. The relatively low degree of substitution of 2-bromoisobutyryl groups can lead to a relatively high graft ratio of PDMAEMA without the occurrence of radical-radical coupling of the propagating chain to form crosslinks due to a high concentration of chain radicals in the local area. According to the FTIR spectrum shown in Fig. 1(d), the chitosan-*g*-PDMAEMA obtained shows new absorption peaks at *ca* 2819 and 2766, 1728 and 1144 cm⁻¹, which are assigned to C-H stretching of the -N(CH₃)₂ group, the carbonyl group and C-N stretching, respectively, which suggests successful grafting. The ¹H NMR spectrum of the graft copolymer is shown in Fig. 2(c). All the proton signals of PDMAEMA graft chains can be observed. The ¹H NMR results confirm the successful preparation of chitosan-*g*-PDMAEMA. In the ¹H NMR spectrum of chitosan-*g*-PDMAEMA the aromatic peaks of the phthalimide are not observed, and in the FTIR spectrum the phthalimide peaks at 721 cm⁻¹ also disappear, which are attributed to the relatively high graft ratio of PDMAEMA.

To investigate the graft ratio, the samples were weighed before and after the graft polymerization with DMAEMA. The graft ratio, *G* (wt%), was calculated according to

$$G = \frac{W_2 - W_1}{W_1} \times 100 \quad (1)$$

where *W*₁ (g) is the weight of chitosan-*g*-Br macroinitiator and *W*₂ (g) is the weight of the chitosan-*g*-PDMAEMA samples.

The results of the ATRP reaction of DMAEMA initiated by the chitosan-Br macroinitiator are listed in Table 1. According to these data, the conversion of DMAEMA and the graft ratio of PDMAEMA increase from 12.7 to 39.4% and from 500 to 1550%, respectively, with an increase of reaction time from 2 to 8 h, indicating that the chitosan-Br macroinitiator has good reaction activity for ATRP. In other words, the chain length of PDMAEMA can be adjusted by variation of the reaction time in this system.

Table 1. Results for ATRP of DMAEMA with chitosan-Br macroinitiator^a

Sample	Reaction time (h)	Conversion (%)	Graft ratio (%) ^b
Chitosan- <i>g</i> -PDMAEMA1	2	12.7	500
Chitosan- <i>g</i> -PDMAEMA2	4	22.1	870
Chitosan- <i>g</i> -PDMAEMA3	5	26.7	1050
Chitosan- <i>g</i> -PDMAEMA4	6	32.1	1260
Chitosan- <i>g</i> -PDMAEMA5	8	39.4	1550

^a Reaction conditions: [DMAEMA]/[chitosan-Br]/[CuBr]/[PMDETA] = 400/1/1/1; reaction temperature = 60 °C.

^b Graft ratio was calculated according to Eqn (1).

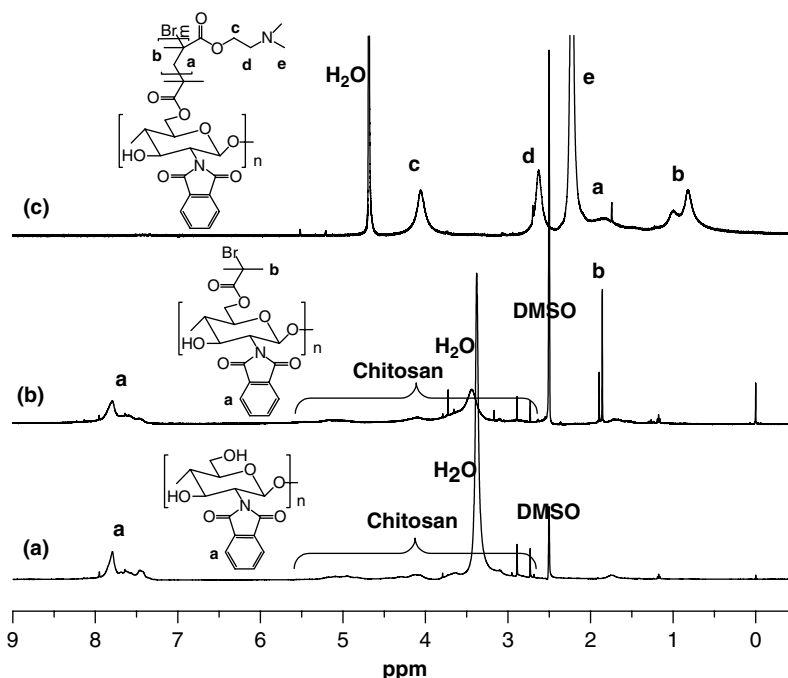


Figure 2. ¹H NMR spectra of (a) phthaloyl-chitosan in DMSO-*d*₆, (b) chitosan-Br in DMSO-*d*₆ and (c) chitosan-*g*-PDMAEMA2 in D₂O.

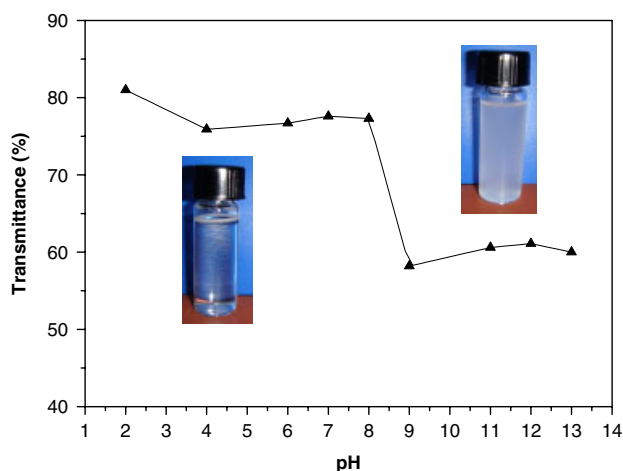


Figure 3. pH dependence of optical transmittance at 500 nm for chitosan-*g*-PDMAEMA2 micelles in water at 20 °C. The concentration of chitosan-*g*-PDMAEMA2 was 15 g L⁻¹.

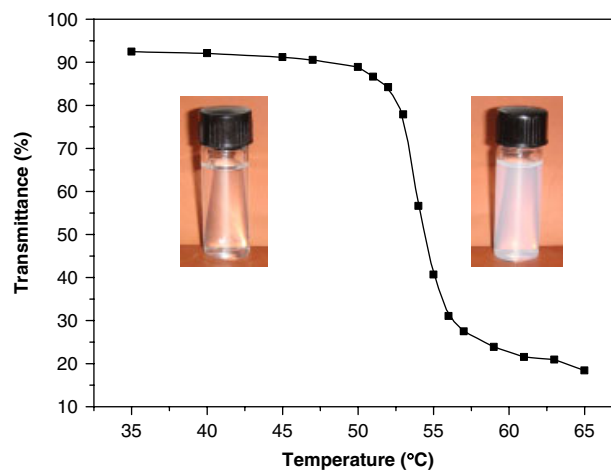


Figure 4. Temperature dependence of optical transmittance at 500 nm for chitosan-*g*-PDMAEMA2 micelles in water (pH = 7). The concentration of chitosan-*g*-PDMAEMA2 was 15 g L⁻¹.

Influence of pH and temperature on chitosan-*g*-PDMAEMA micelles

Chitosan-*g*-PDMAEMA micelles were formed by the dissolution of the copolymer in water. The pH- and temperature-sensitive characteristics of copolymer micelles were investigated using UV-visible spectroscopy and DLS. Figure 3 shows the pH dependence of optical transmittance at 500 nm for chitosan-*g*-PDMAEMA micelles in water. With an increase of pH, the solution transforms sharply from transparent to opaque, indicating the obvious pH-responsive property of PDMAEMA graft chains. Figure 4 shows the temperature dependence of optical transmittance at 500 nm for chitosan-*g*-PDMAEMA micelles in neutral aqueous solution. With increasing temperature, the solution transforms sharply from transparent to opaque. It is a typical LCST (about 53 °C)

of temperature-responsive PDMAEMA graft chains. These optical transmittance measurements show that chitosan-*g*-PDMAEMA has pH- and temperature-responsive properties.

DLS was used to measure the size of chitosan-*g*-PDMAEMA micelles in aqueous solution at various pH values and temperatures, and the results are shown in Figs 5 and 6, respectively. According to Fig. 5, with an increase of pH, the hydrodynamic radius (*R*_h) decreases from 415.8 to 136.5 nm, indicating the pH-responsive behavior of chitosan-*g*-PDMAEMA due to the protonation/deprotonation of *N,N*-dimethylaminoethyl groups in PDMAEMA chains. With increasing pH, PDMAEMA chains shrink gradually from a stretched conformation, which leads to a decrease in the size of the copolymer micelles. However, the influence of temperature on the copolymer micelles (Fig. 6) is somewhat

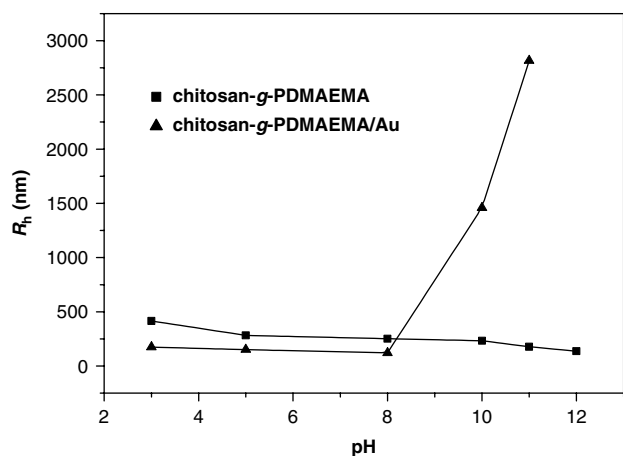


Figure 5. Variation of average hydrodynamic radius, R_h , of original micelles and hybrid micelles as a function of pH at 20 °C. The concentration of chitosan-*g*-PDMAEMA2 was 4 g L⁻¹.

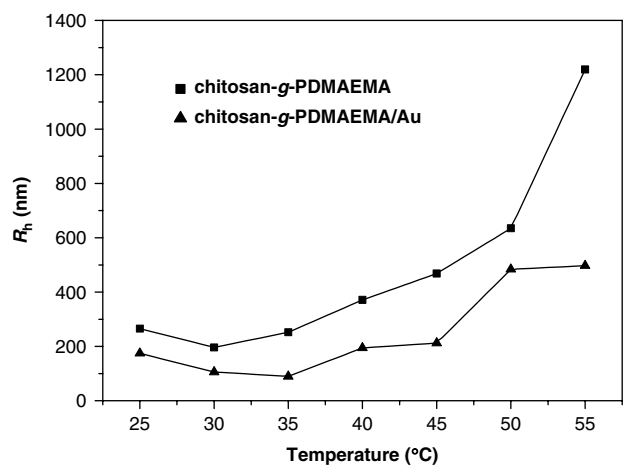


Figure 6. Variation of average hydrodynamic radius, R_h , of original micelles and hybrid micelles as a function of temperature (pH = 7). The concentration of chitosan-*g*-PDMAEMA2 was 2 g L⁻¹.

different from that of pH. In the lower temperature range from 25 to 35 °C, R_h varies slightly; however, the value increases markedly in the temperature range from 35 to 55 °C. This can be explained by the change in conformation of PDMAEMA chains. At lower temperatures, PDMAEMA chains in the chitosan-*g*-PDMAEMA copolymer present a random coil conformation due to the hydrogen bonding interactions between polymer chains and water molecules. As the temperature increases to a critical value, the polymer chains shrink into a globular conformation owing to the hydrophobic interactions between *N,N*-dimethylaminoethyl groups. In this condition, the micelles with a shrunken PDMAEMA corona tend to group together into nano-aggregates with greater sizes. With increasing temperature, the size measured by DLS increases until micrometer-sized colloidal particles are formed.

Stabilization of Au NPs by chitosan-*g*-PDMAEMA graft copolymer micelles

For the stabilization of Au NPs by copolymer micelles, an aqueous solution of chitosan-*g*-PDMAEMA was first treated with HAuCl₄ solution, and the reduction to Au NPs was achieved by addition of excess aqueous solution of NaBH₄. The solution immediately

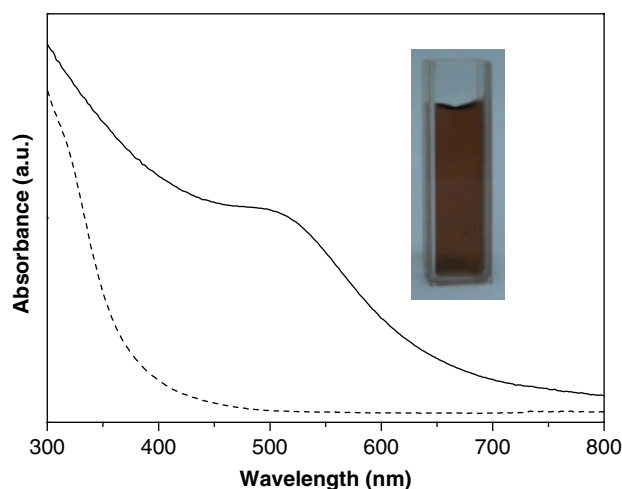


Figure 7. UV-visible absorption spectra of chitosan-*g*-PDMAEMA2/HAuCl₄ mixed solutions before (dashed curve) and after (solid curve) reduction with NaBH₄. The concentration of chitosan-*g*-PDMAEMA2 was 0.23 g L⁻¹.

turned red-brown. Figure 7 shows the UV-visible absorption spectra before and after reduction. After the addition of NaBH₄, the absorption spectrum displays a significant surface plasmon band at 519 nm. This band is characteristic of metallic gold colloids with a diameter of about 10 nm, indicating the formation of Au NPs.^{58–60} The hybrid micelles prepared incorporating Au NPs are highly stable at room temperature, and no precipitation is observed over a period of more than 8 weeks. The stability of the Au NPs over long storage times confirms the nanoparticles are stabilized inside the PDMAEMA corona of the copolymer micelles.

Influence of pH and temperature on chitosan-*g*-PDMAEMA/Au hybrid micelles

The pH- and temperature-sensitive characteristics of chitosan-*g*-PDMAEMA/Au hybrid micelles were investigated using DLS. Figure 5 shows the pH dependence of R_h of the hybrid micelles. At lower pH (≤ 8), the size of the hybrid micelles is smaller than that of the original chitosan-*g*-PDMAEMA micelles. This suggests the quite strong complexation of Au NPs to the PDMAEMA corona and the fact that the nanoparticles act as physical crosslinkers of the corona. At higher pH (> 8), the R_h value increases rapidly. Obviously, for strongly basic conditions, the corona of the hybrid micelles collapses and intermicellar aggregation occurs at a high concentration of 2 g L⁻¹, which leads to the formation of micrometer-sized colloidal particles.

Figure 6 shows the temperature dependence of R_h of the hybrid micelles. The variation of R_h of the hybrid micelles is similar to that of the original micelles. However, there are some differences between the two types of micelles. The size of the hybrid micelles is smaller than that of the original micelles in the whole temperature range due to the strong complexation of Au NPs to the PDMAEMA corona. In particular, at higher temperatures, the hybrid micelles aggregate into larger particles but the size is much smaller than that of aggregates of the original micelles. This result reflects that the incorporation of Au NPs partially restricts the collapse at higher temperatures. Therefore, the intermicellar aggregation of the hybrid micelles is weaker than that of the original micelles.

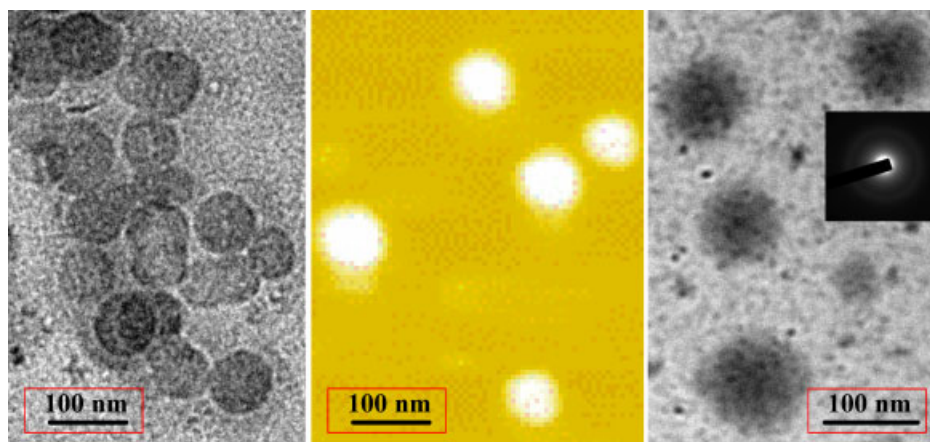


Figure 8. TEM images of chitosan-*g*-PDMAEMA2 micelles (left) and chitosan-*g*-PDMAEMA2/Au hybrid micelles (right; the inset shows the electron diffraction of Au in the hybrid micelles) and AFM image of chitosan-*g*-PDMAEMA2 micelles (center).

Morphology of chitosan-*g*-PDMAEMA micelles and chitosan-*g*-PDMAEMA/Au hybrid micelles

The morphology of the chitosan-*g*-PDMAEMA micelles and chitosan-*g*-PDMAEMA/Au hybrid micelles was examined using TEM and AFM. As shown in Fig. 8, the original and hybrid micelles are relatively uniform and the sizes of them range from 60 to 100 nm. It can be seen from the left-hand image of Fig. 8 that the chitosan-*g*-PDMAEMA2 copolymer can self-assemble into stable and uniform micelles in water. The AFM image (central image of Fig. 8) further confirms that the graft copolymers can form uniform spherical micelles. The hybrid micelles of chitosan-*g*-PDMAEMA2/Au are shown in the right-hand image of Fig. 8. The size of Au NPs is about 10 nm, in accordance with the results of analysis of the UV-visible absorption spectrum of the original Au NPs. Almost all Au NPs are located on the copolymer micelles although a few Au NPs spread out of the micelles, which indicates that the PDMAEMA corona of micelles acts as the ‘nanoreactor’ and ‘anchor’ for the *in situ* formation and stabilization of the Au NPs. Moreover, no aggregation of Au NPs stabilized onto PDMAEMA chains occurs; therefore, the spatial distribution of Au NPs within micelles can be tuned by variation of the micelle conformation due to the pH- and temperature-sensitive responses of PDMAEMA chains.

CONCLUSIONS

A series of chitosan-*g*-PDMAEMA graft copolymers were synthesized successfully by ATRP of DMAEMA under mild conditions. The copolymers can form stable spherical micelles in water. Au NPs were then embedded into the pH- and temperature-responsive micelles via *in situ* formation and stabilization to form stable chitosan-*g*-PDMAEMA/Au hybrid micelles. The PDMAEMA corona acts as the ‘nanoreactor’ and ‘anchor’ during the process. The spatial distribution of Au NPs in the micelles can be tuned conveniently by variation of temperature and pH of the external surroundings. In this way, the stabilized Au NPs can act as an indicator of external conditions. For example, the hybrid micelles could be used as a chemical or biomedical monitor of a specific chemical or biochemical species. Moreover, the hybrid micelles can be used as a ‘nanoreactor’ in the field of catalysis, and the permeability of the PDMAEMA corona to reactants can be adjusted through the variation of temperature or pH. Chitosan is an important natural biomaterial and Au NPs have significant applications

in biomedicine. Therefore, the chitosan/Au NP hybrid micelles have potential biomedical applications in biocatalysis, biosensors and biotesting.

ACKNOWLEDGEMENT

The authors gratefully acknowledge the financial support of the National Natural Science Foundation of China (no. 20804029).

REFERENCES

- 1 Taton TA, Mirkin CA and Letsinger RL, *Science* **289**:1757–1760 (2000).
- 2 Campbell CT, Parker SC and Starr DE, *Science* **298**:811–814 (2002).
- 3 Lewis LN, *Chem Rev* **93**:2693–2730 (1993).
- 4 Daniel MC and Astruc D, *Chem Rev* **104**:293–346 (2004).
- 5 Zhao M and Crooks RM, *Angew Chem Int Ed* **38**:364–366 (1999).
- 6 Maier SA, Brongersma ML, Kik PG, Meltzer S, Requicha AAG and Atwater HA, *Adv Mater* **13**:1501–1505 (2001).
- 7 Chen SW and Yang YY, *J Am Chem Soc* **124**:5280–5281 (2002).
- 8 Krämer S, Xie H, Gaff J, Williamson JR, Tkachenko AG, Nouri N, *et al*, *J Am Chem Soc* **126**:5388–5395 (2004).
- 9 Ivanisevic A and Kinsella JM, *J Am Chem Soc* **127**:3276–3277 (2005).
- 10 Gao JH, Zhang W, Huang PB, Zhang B, Zhang XX and Xu B, *J Am Chem Soc* **130**:3710–3711 (2008).
- 11 Peng XG and Xiao M, *Nano Lett* **3**:819–822 (2003).
- 12 You CC, Verma AV and Rotello M, *Soft Matter* **2**:190–204 (2006).
- 13 Lopes WA and Jaeger HM, *Nature* **414**:735–738 (2001).
- 14 Hammond PT, *Adv Mater* **16**:1271–1293 (2004).
- 15 Tang Z and Kotov NA, *Adv Mater* **17**:951–962 (2005).
- 16 Elbjairami O and Omary MA, *J Am Chem Soc* **129**:11384–11393 (2007).
- 17 Mukherjee P, Patra CR, Ghosh A, Kumar R and Sastry M, *Chem Mater* **14**:1678–1684 (2002).
- 18 Alric C, Taleb J, Le Duc G, Mandon C, Billotey C, Le Meur-Herland A, *et al*, *J Am Chem Soc* **130**:5908–5915 (2008).
- 19 Chithrani BD, Ghazani AA and Chan WCW, *Nano Lett* **6**:662–668 (2006).
- 20 Liu XL, Dai Q, Austin L, Coutts J, Knowles G, Zou JH, *et al*, *J Am Chem Soc* **130**:2780–2782 (2008).
- 21 Shifrina ZB, Rajadurai MS, Firsova NV, Bronstein LM, Huang X, Rusanov AL, *et al*, *Macromolecules* **38**:9920–9932 (2005).
- 22 Worden JG, Dai Q and Huo Q, *Chem Commun* 1536–1538 (2006).
- 23 Chen CW, Chen MQ, Serizawa T and Akashi M, *Adv Mater* **10**:1122–1126 (1998).
- 24 Cen L, Neoh KG and Kang ET, *Adv Mater* **17**:1656–1656 (2005).
- 25 Lu Y, Mei Y, Drechsler M and Ballauff M, *Angew Chem Int Ed* **45**:813–816 (2006).
- 26 Zhang JG, Xu SQ and Kumacheva E, *J Am Chem Soc* **126**:7908–7914 (2004).
- 27 Zhang JG, Xu SQ and Kumacheva E, *Adv Mater* **17**:2336–2340 (2005).
- 28 Pich A, Hain J, Lu Y, Boyko V, Prots Y and Adler H-J, *Macromolecules* **38**:6610–6619 (2005).

- 29 Kang Y and Taton TA, *Angew Chem Int Ed* **44**:409–412 (2005).
- 30 Zhao H and Douglas EP, *Chem Mater* **14**:1418–1423 (2002).
- 31 Liu SY, Weaver JVM, Save M and Armes SP, *Langmuir* **18**:8350–8357 (2002).
- 32 Filali M, Meier MAR, Schuber US and Gohy JF, *Langmuir* **21**:7995–8000 (2005).
- 33 Xu HX, Xu J, Zhu ZY, Liu HW and Liu SY, *Macromolecules* **39**:8451–8455 (2006).
- 34 Gupta S, Uhlmann P, Agrawal M, Chapuis S, Oertel U and Stamm M, *Macromolecules* **41**:2874–2879 (2008).
- 35 Gupta S, Agrawal M, Uhlmann P, Simon F, Oertel U and Stamm M, *Macromolecules* **41**:8152–8158 (2008).
- 36 Chen X, An YL, Zhao DY, He ZP, Zhang Y, Cheng J, *et al*, *Langmuir* **24**:8198–8204 (2008).
- 37 Zheng PW, Jiang XW, Zhang X, Zhang WQ and Shi LQ, *Langmuir* **22**:9393–9396 (2006).
- 38 Hou GL, Zhu L, Chen DY and Jiang M, *Macromolecules* **40**:2134–2140 (2007).
- 39 Dockendorff J, Gauthier M, Mourran A and Möller M, *Macromolecules* **41**:6621–6623 (2008).
- 40 Zhang MM, Liu L, Wu CL, Fu GQ, Zhao HY and He BL, *Polymer* **48**:1989–1997 (2007).
- 41 Li YT, Smith AE, Lokitz BS and McCormick CL, *Macromolecules* **40**:8524–8526 (2007).
- 42 Rutnakornpituk M and Ngamdee P, *Polymer* **47**:7909–7917 (2006).
- 43 Liu L, Chen LX and Fang YE, *Macromol Rapid Commun* **27**:1988–1994 (2006).
- 44 Chung HJ, Bae JW, Park HD, Lee JW and Park KD, *Macromol Symp* **224**:275–286 (2005).
- 45 Fujioka M, Okada H, Kusaka Y, Nishiyama S, Noguchi H, Ishii S, *et al*, *Macromol Rapid Commun* **25**:1776–1780 (2004).
- 46 Laudenslager MJ, Schiffman JD and Schauer CL, *Biomacromolecules* **9**:2682–2685 (2008).
- 47 Heinemann C, Heinemann S, Bernhardt A, Worch H and Hanke T, *Biomacromolecules* **9**:2913–2920 (2008).
- 48 Skotak MS, Leonov AP, Larsen G, Noriega S and Subramanian A, *Biomacromolecules* **9**:1902–1908 (2008).
- 49 Lallana E, Fernandez-Megia E and Riguera R, *J Am Chem Soc* **131**:5748–5750 (2009).
- 50 Strand SP, Issa MM, Christensen BE, Vårum KM and Artursson P, *Biomacromolecules* **11**:3268–3276 (2008).
- 51 Jenkins DW and Hudson SM, *Macromolecules* **35**:3413–3419 (2002).
- 52 Qian F, Cui FY, Ding JY, Tang C and Yin CH, *Biomacromolecules* **7**:2722–2727 (2006).
- 53 Recillas M, Silva LL, Peniche C, Goycoolea FM, Rinaudo M and Argüelles-Monal WM, *Biomacromolecules* **10**:1633–1641 (2009).
- 54 Feng H and Dong CM, *J Polym Sci A: Polym Chem* **44**:5353–5361 (2006).
- 55 Feng H and Dong CM, *Biomacromolecules* **7**:3069–3075 (2006).
- 56 Yu HJ, Chen XS, Lu TC, Sun J, Tian HY, Hu J, *et al*, *Biomacromolecules* **8**:1425–1435 (2007).
- 57 Li N, Bai RB and Liu CK, *Langmuir* **21**:11780–11787 (2005).
- 58 Brown KR, Walter DG and Natan MJ, *Chem Mater* **12**:306–313 (2000).
- 59 Grabar KC, Freeman RG, Hommer MB and Natan MJ, *Anal Chem* **67**:735–743 (1995).
- 60 Xu HX, Xu J, Jiang XZ, Zhu ZY, Rao JY, Yin J, *et al*, *Chem Mater* **19**:2489–2494 (2007).